Kinetics and Mechanism of Hydrolysis of Aflatoxin B_1 *exo*-8,9-Epoxide and Rearrangement of the Dihydrodiol

William W. Johnson, Thomas M. Harris, and F. Peter Guengerich*

Contribution from the Departments of Biochemistry and Chemistry and the Center in Molecular Toxicology, Vanderbilt University, Nashville, Tennessee 37232

Received February 20, 1996[⊗]

Abstract: Aflatoxin B_1 (AFB_1) is thought to play a large role in human liver cancer in some parts of the world, and the mechanism of genotoxicity is generally considered to involve the DNA adduct formed at the guanyl N7 atom. The *exo* epoxide, the genotoxic isomer formed by human cytochrome P450 3A4, has been known to be very unstable in H_2O ($t_{1/2} < 10$ s). The rates of hydrolysis of AFB_1 *exo* epoxide have been determined as a function of pH using stopped flow kinetics. The spontaneous reaction with solvent is faster than previously suspected, with a $t_{1/2} \sim 1$ s when either absorbance or fluorescence kinetic traces are measured at ambient temperature. An acid-catalyzed reaction with a bimolecular rate constant of 2×10^3 M^{-1} s^{-1} is operative below about pH 5 and elevates the rate. The hydrolysis product, AFB diol, reversibly converts to a furofuran-ring-opened oxyanionic AFB_1 α-hydroxydialdehyde (AFB dialdehyde) under slightly basic conditions. When AFB diol was treated with base in DMSO, conversion to AFB dialdehyde was accompanied by dehydration of the remaining alcohol group. In aqueous solution, the AFB diol:AFB dialdehyde equilbrium has been characterized and the pK_a (8.2) is much higher than previously suggested; the base-catalyzed bimolecular rate of 2.3×10^3 M^{-1} s^{-1} results in a very slow rate of conversion at physiological pH. Multiphasic conversion of AFB dialdehyde back to AFB diol has a slow rate-limiting step at 0.01 s^{-1} and is nearly quantitative. The dehydrated AFB dialdehyde formed in DMSO did not form a detectable ring closed derivative.

Introduction

Exposure to the mycotoxin aflatoxin B_1 (AFB_1) is generally considered to play a major role in human liver cancer in some parts of the world.[1−3] Aflatoxins are a group of difurano-coumarin compounds produced by the common fungal molds *Aspergillus flavus*, *A. parasiticus*, and *A. nomius*, which grow in hot moist conditions on agricultural commodities.[4] AFB_1 is among the most potent mutagens implicated in human carcinogenesis.[5] Metabolic activation to the *exo*-8,9-epoxide results in a very reactive electrophile, which forms adducts with the N7 position of guanine residues in DNA.[6] The *endo* epoxide has been shown to be about 40-fold more stable in H_2O than the *exo* and is unreactive with DNA and essentially non-genotoxic.[7] While cytochromes P450 1A2 and 2A6 and cooxidation by peroxide products of lipoxygenase and prostaglandin synthase can produce the epoxide, cytochrome P450 3A4 is the major human liver enzyme involved in AFB_1 activation and produces essentially only the genotoxic *exo* isomer.[8] The *exo* epoxide also reacts very rapidly with H_2O with a suspected half-life of <10 s (Scheme 1)[7,9,10] and is one of the most reactive of all biologically relevant epoxides. However, it is inert to acetone and other aprotic, nonnucleophilic solvents. Consequently, many experiments with the *exo* epoxide have required solvents such as CH_2Cl_2 or acetone.[7]

Scheme 1. Reaction Pathway of AFB_1 8,9-Epoxide in Cytosolic Environment.

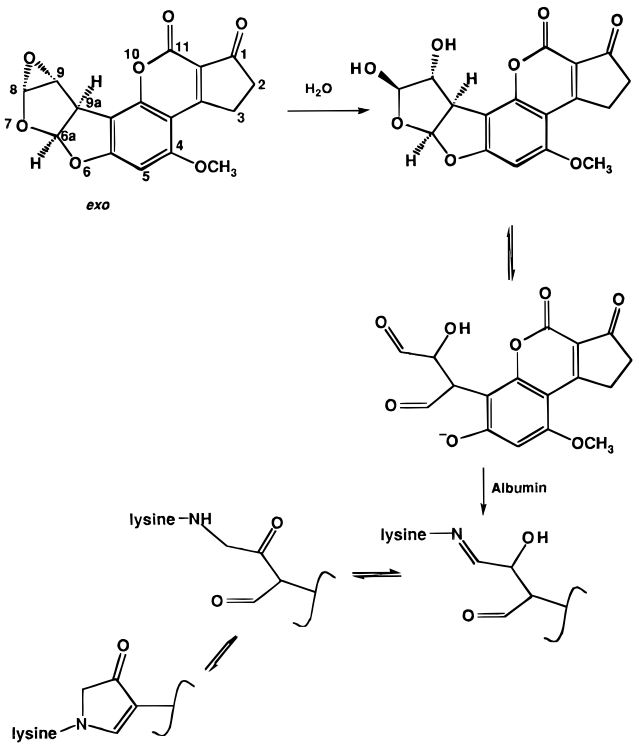

Detoxication of the AFB_1 epoxide by the enzyme epoxide hydrolase has been suggested[11,12] but definite conclusions

[⊗] Abstract published in *Advance ACS Abstracts*, August 1, 1996.

(1) Busby, W. F.; Wogan, G. N. In *Chemical Carcinogens*; Searle, C. E., Ed.; American Chemical Society: Washington, DC, 1984; pp 945−1136.
(2) Groopman, J. D.; Cain, L. G.; Kensler, T. W. *Crit. Rev. Toxicol.* **1988**, *19*, 113−145.
(3) Wogan, G. N. *Cancer Res.* **1992**, Suppl. 52: 2114s−2118s.
(4) Massey, T. E.; Stewart, R. K.; Daniels, J. M.; Liu, L. *Proc. Exp. Biol. Med.* **1995**, *208*, 213−227.
(5) Garner, R. C.; Wright, C. M. *Br. J. Cancer* **1973**, *28*, 544−551.
(6) Raney, V. M.; Harris, T. M.; Stone, M. P. *Chem. Res. Toxicol.* **1993**, *6*, 64−68.
(7) Iyer, R.; Coles, B.; Raney, K. D.; Thier, R.; Guengerich, F. P.; Harris, T. M. *J. Am. Chem. Soc.* **1994**, *116*, 1603−1609.
(8) Ueng, Y-F.; Shimada, T.; Yamazaki, H.; Guengerich, F. P. *Chem. Res. Toxicol.* **1995**, *8*, 218−225.
(9) Gopalakrishnan, S.; Harris, T. M.; Stone, M. P. *Biochemistry* **1990**, *29*, 10438−10448.
(10) Baertschi, S. W.; Raney, K. D.; Shimada, T.; Harris, T. M.; Guengerich, F. P. *Chem. Res. Toxicol.* **1989**, *2*, 114−122.

S0002-7863(96)00525-2 CCC: $12.00

regarding this hypothesis are not available. The instability of AFB_1 *exo*-8,9-epoxide in protic solvents makes direct measurement of the enzymatic reaction difficult. Rates of hydrolysis via epoxide hydrolase are commonly moderate even though this enzyme, like many detoxication enzymes, has a high affinity for lipophilic chemicals and can be very efficient.[13] Consequently, a proposed role for epoxide hydrolase with such an unstable epoxide as this one is tenuous. Goals of this study were to determine the rates of reaction of the AFB_1 *exo*-8,9-epoxide with H_2O and the mechanisms as they relate to the availability of protons in light of the proposed proton-rich microenvironment near DNA.[14,15]

Some spectral characteristics of the hydrolyzed product of the epoxide, 8,9-dihydro-8,9-dihydroxy AFB_1 (AFB diol), and a close analog, AFB_{2a},[16] are known. The absorbance spectra of AFB_{2a}[17] and AFB diol have λ_{max} at 365 nm in CH_3OH.[18] Fluorescence has been used for detection of acid-hydrolyzed AFB_1[19] or AFB_1-DNA adducts.[20] However, neither the absorbance nor fluorescence spectrum of AFB_1 diol in H_2O has been reported. Additionally, neither the absorbance nor the fluorescence spectrum of AFB_1 epoxide has been reported in any medium, due to the difficulty in obtaining AFB_1 epoxide, a problem which was surmounted by the development of a synthetic method using an aprotic medium.[21]

AFB diol is generally believed to reversibly convert to a furofuran ring-opened oxyanionic form, α-hydroxydialdehyde AFB_1 (AFB dialdehyde), in slightly basic conditions (Scheme 1).[16,17] This conversion is shown by the reversible bathochromic shift caused by the phenolate, an anion that can reside on the other two carbonyl oxygens through resonance. AFB dialdehyde forms Schiff bases with primary amine groups leading to protein adducts.[17,22−24] Indeed, the very close analog of the AFB diol, AFB_{2a} (aflatoxin hemiacetal), binds rapidly to protein at pH 7.4.[17] The *in vivo* lysine adduct in serum albumin formed from AFB dialdehyde has been characterized.[22] A single molecule of tris(hydroxymethyl)methylamine (Tris) reacts with the AFB dialdehyde arising from AFB dihydrodiol,[25] indicating that the terminal aldehyde is the strongly preferred electrophile. The AFB diol has been shown to be an inhibitor of protein synthesis in an *in vitro* system.[24] Moreover, an aldehyde reductase with activity toward AFB dialdehyde has been associated with resistance to the cytotoxicity of AFB_1.[26−28] Therefore, the hydrolysis product appears to contribute to the cytotoxic action of AFB_1 and the AFB dialdehyde may be of some significance. The pK_a for the conversion of AFB diol to AFB dialdehyde has been suggested to be about 7.0−7.4 based on studies with the hemiacetal analog AFB_{2a}.[17] The liver cell environment is about pH 7.5,[29] and the hydrolyzed AFB_1 epoxide has been believed to be largely in the dialdehyde form. Therefore, another objective of this study was determination of the rates and pH dependence of the diol/dialdehyde conversion as well as the mechanism.

Our present studies show that the rate of spontaneous hydrolysis of AFB_1 *exo*-8,9-epoxide is even faster than previously suspected and that an acid-catalyzed reaction elevates the rate at pH <5. The spontaneous reaction has a $t_{1/2}$ of ∼1 s and the acid-catalyzed bimolecular rate was determined. The subsequent base-catalyzed conversion of the diol to the dialdehyde was also characterized. The reverse reaction to the diol is multi-phasic and has a rate-limiting step occurring at 0.01 s^{-1}; the pK_a of this equilibrium is higher than expected (8.2).

Experimental Section

Chemicals. AFB_1 8,9-epoxide was synthesized by treatment of AFB_1 (Sigma Chemical Co., St. Louis, MO) with 1.5 equiv of dimethyldioxirane[21] producing a mixture of *exo* and *endo* isomers in a ration of 9:1, as judged by ^{1}H NMR.[30] The *exo* isomer of AFB_1 8,9-oxide was purified by recrystallization from a solution of anhydrous CH_2Cl_2/$(CH_3)_2CO$ (1:1 v/v) at −20 °C for 24 h.[30]

Spectroscopy. Absorbance spectra were recorded with a Cary 14/OLIS spectrophotometer (On-Line Instrument Systems, Bogart, GA). Absorbance spectra of AFB_1 8,9-epoxide were measured in anhydrous $(CH_3)_2CO$ and those of AFB_1 diol in buffer at pH 3. Fluorescence spectra were recorded with a Varian SF-330 spectrofluorometer (Varian, Walnut Creek, CA), with AFB diol at 0.47 μM and the epoxide at 47 μM. The data from the pH titration of the AFB diol:AFB dialdehyde equilibrium were analyzed by curve fitting to a sigmoidal function $y = [\lim 10 \exp(\mathrm{pH} - \mathrm{p}K_a)]/[10 \exp(\mathrm{pH} - \mathrm{p}K_a) + 1]$, with GraFit (Robin Leatherbarrow, Erithacus Software Limited, UK).

Hydrolysis Kinetics. Stopped-flow measurements utilized an apparatus designed and built by Applied Photophysics Ltd. (Leatherhead, UK). This apparatus has a 1.3 ms dead time, 2 and 10 mm path lengths, and a thermostated observation cell (maintained at 25 °C in this case). Data are collected by a computer programmed to collect data over a given time interval following a trigger impulse a few milliseconds before stop. Data analysis software is standard and implements a Marquardt-Levenberg algorithm for nonlinear regression analysis of traces to analytical equations. At least eight reactions were averaged for data analysis in most experiments. Repetitive scans were acquired with an Applied Photophysics photodiode array using a linear 256-element diode array with wavelength separation of 3.3 nm and a maximum speed of 2.56 ms/scan.

The hydrolysis of AFB_1 epoxide was performed by rapidly mixing, in the stopped flow apparatus, AFB_1 *exo*-8,9-epoxide in anhydrous $(CH_3)_2CO$ with buffer in a volumetric ratio of 1:10 by replacing one of the syringes with one of 0.1× volume, resulting in a final $(CH_3)_2CO$ concentration of 9%. The final concentration of AFB1 *exo*-8,9-epoxide was 7 μM. In experiments to determine the relationship of rate to pH experiments, the following buffer salts were used at 5 mM: sodium glycine, pK_a 2.3; sodium ethylenediaminetetraacetate (EDTA), pK_a 2.6; sodium formate, pK_a 3.8; KH_2PO_4, pK_a 4.3; sodium citrate,

(11) Ch'ih, J. J.; Lin, T.; Devlin, T. M. *Biochem. Biophys. Res. Commun.* **1983**, *110*, 668−674.
(12) McGlynn, K. A.; Rosvold, E. A.; Lustbader, E. D.; Hu, Y.; Clapper, M. L.; Zhou, T.; Wild, C. P.; Xia, X-L.; Baffoe-Bonnie, A.; Ofori-Adjei, D.; Chen, G-C.; London, W. T.; Shen, F-M.; Buetow, K. H. *Proc. Natl. Acad. Sci. U.S.A.* **1995**, *92*, 2384−2387.
(13) Armstrong, R. N. *Crit. Rev. Biochem.* **1987**, *22*, 39−88.
(14) Islam, N. B.; Whalen, D. L.; Yagi, H.; Jerina, D. M. *J. Am. Chem. Soc.* **1987**, *109*, 2108−2111.
(15) Lamm, G.; Pack, G. R. *Proc. Natl. Acad. Sci. U.S.A.* **1990**, *87*, 9033−9030.
(16) Büchi, G.; Foulkes, D. M.; Kurono, M.; Mitchell, G. F.; Schneider, R. S. *J. Am. Chem. Soc.* **1967**, *89*, 6745−6753.
(17) Patterson, D. S. P.; Roberts, B. A. *Fd Cosmet. Toxicol.* **1970**, *8*, 527−538.
(18) Swenson, D. H.; Miller, J. A.; Miller, E. C. *Biochem. Biophys. Res. Commun.* **1973**, *53*, 1260−1267.
(19) Ciegler, A.; Peterson, R. E. *Appl. Microbiol.* **1968**, *16*, 665−666.
(20) Lin, J. K.; Miller, J. A.; Miller, E. C. *Cancer Res.* **1977**, *37*, 4430−4438.
(21) Baertschi, S. W.; Raney, K. D.; Stone, M. P.; Harris, T. M. *J. Am. Chem. Soc.* **1988**, *110*, 7929−7931.
(22) Sabbioni, G.; Skipper, P. L.; Büchi, G.; Tannenbaum, S. R. *Carcinogenesis* **1987**, *8*, 819−824.
(23) Sabbioni, G.; Wild, C. P. *Carcinogenesis* **1991**, *12*, 97−103.
(24) Neal, G. E.; Judah, D. J.; Stirpe, F.; Patterson, D. S. P. *Toxicol. Appl. Pharmacol.* **1981**, *58*, 431−437.
(25) Coles, B. F.; Welch, A. M.; Hertzog, P. J.; Lindsay Smith, J. R.; Garner, R. C. *Carcinogenesis* **1980**, *1*, 79−90.
(26) Hayes, J. D.; Judah, D. J.; Neal, G. E. *Cancer Res.* **1993**, *53*, 3887−3894.
(27) Ellis, E. M.; Judah, D. J.; Neal, G. E.; Hayes, J. D. *Proc. Natl. Acad. Sci. U.S.A.* **1993**, *90*, 10350−10354.
(28) Judah, D. J.; Hayes, J. D.; Yang, J.-C.; Lian, L.-Y.; Roberts, G. C. K.; Farmer, P. B.; Lamb, J. H.; Neal, G. E. *Biochem. J.* **1993**, *292*, 13−18.
(29) Guyton, A. C. *Textbook of Medical Physiology*; W. B. Saunders Company: Philadelphia, 1991.
(30) Raney, K. D.; Coles, B.; Guengerich, F. P.; Harris, T. M. *Chem. Res. Toxicol.* **1992**, *5*, 333−335.

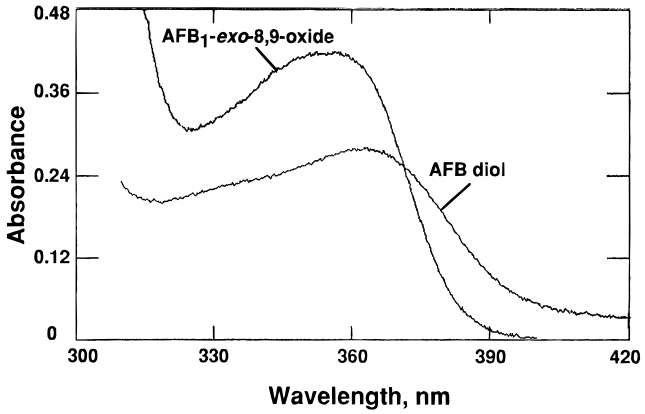

Figure 1. UV spectra of AFB_1 8,9-epoxide and AFB diol. The spectrum of AFB_1 *exo*-8,9-epoxide (11.7 μM) was recorded in anhydrous $(CH_3)_2CO$ (λ_{max} 350 nm). The spectrum of AFB diol (11.7 μM) was measured in pH 5.7 buffer (λ_{max} 365 nm).

pK_a 4.7 and 5.4; sodium 2-[*N*-morpholino]ethanesulfonate (MES), pK_a 6.2; EDTA, pK_a 6.3; sodium *N*-[2-acetamido]-2-iminodiacetate (ADA), pK_a 6.6; sodium 3-[*N*-morpholino]-2-hydroxypropanesulfonate (MOPS), pK_a 7.2; sodium *N*-(2-hydroxyethyl)-piperazine-*N*′-(2-ethanesulfonate) (HEPES), pK_a 7.5; sodium *N*-tris(hydroxymethyl)methylglycine (TRICINE), pK_a 8.2; sodium *N*,*N*-bis(2-hydroxyethyl)glycine (BICINE), pK_a 8.4; sodium *N*-(tris(hydroxymethyl)methyl)-3-aminopropanesulfonate (TAPS), pK_a 8.4; K_2HPO_4, pK_a 9.0; sodium 2-(*N*-cyclohexylamino)-ethanesulfonate (CHES), pK_a 9.3; sodium 3-(cyclohexylamino)-1-propanesulfonate (CAPS), pK_a 10.4; and EDTA, pK_a 10.6.

HPLC of AFB Diol and Reconverted AFB Diol. HPLC methods were as described elsewhere.[31] AFB diol was added to pH 9.9 buffer for various times and then acidified with CH_3CO_2H; 50 μL aliquots of 73 μM product were injected on HPLC and the eluent was monitored at 365 nm.

NMR. ^{1}H NMR specta were recorded on a Bruker AM 400 spectrometer at 400.13 MHz and 27 °C. Samples were prepared in "100%" DMSO-d_6 (Aldrich Chemical Co., Milwaukee, WI).

Results

Absorbance Changes. Characterization of the spectral features of the AFB_1 *exo*-8,9-epoxide and AFB diol was necessary to determine any distinctions between the reactant and the product for observation over time. The absorbance spectra (Figure 1) indicate a λ_{max} of 350 nm for the epoxide and λ_{max} of 365 nm for the hydrolysis product, AFB_1 diol. A comparison of the spectra indicates that the largest change in absorbance upon hydrolysis of the epoxide is between 370 and 390 nm. Indeed, the diode array spectra (Figure 2) of epoxide hydrolysis collected over 8 s show the largest change at about 386 nm, which was the wavelength used thereafter for single wavelength kinetics experiments (e.g., Figure 3). The data (Figure 3) fit very well to a single exponential analysis equation with the random error variance remaining constant over the reaction time. The observed rate for this event was 0.66 s^{-1} at 25 °C.

Fluorescence Change. The difference in the fluorescence spectra between the epoxide and the hydrolysis product is very large (Figure 4). The excitation wavelength for all of these spectra was at 328 nm; the excitation maximum for the hydrolysis product was found to be 367 nm. The concentration of the epoxide is 10-fold higher than for the diol, and the scale is expanded in Figure 4; hence, the elevation in fluorescence at 452 nm is nearly 10^3-fold upon hydrolysis of the epoxide and provides an excellent signal to monitor during stopped-flow kinetic experiments (Figure 5). The observed rate of 0.60 s^{-1} is in agreement with the absorbance experiments.

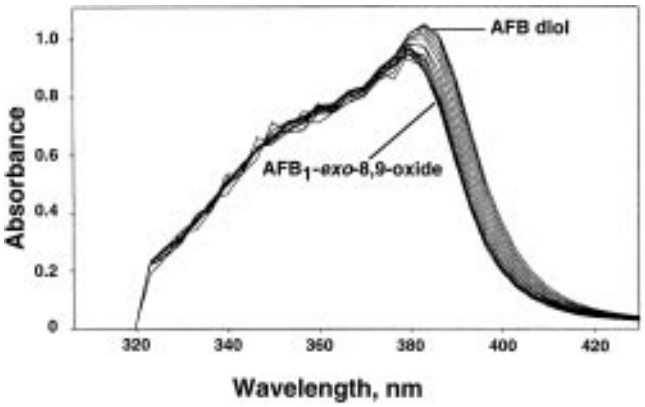

Figure 2. Photodiode array-acquired spectra of the hydrolysis of AFB_1 *exo*-8,9-epoxide. Spectra were recorded every 2.56 ms over 8 s, referenced against buffer. Only every 20th spectrum is displayed. The reaction concentration of AFB_1 *exo*-8,9-epoxide was 400 μM.

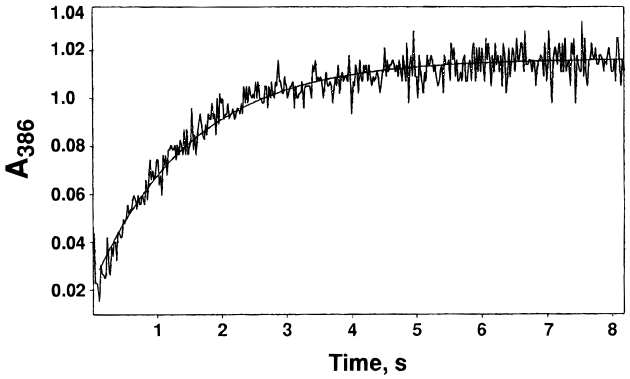

Figure 3. Time-dependent A_{386} change during the hydrolysis of AFB_1 *exo*-8,9-epoxide. The curve fit to the data is a single exponential equation $Y = A_o e^{-kt} + B$, where k is k_{obs} (0.66 ± 0.0001 s^{-1}). The reaction was in pH 7.0 buffer (25 °C) with 400 μM AFB_1 *exo*-8,9-epoxide and 9% (v/v) $(CH_3)_2CO$ (after mixing).

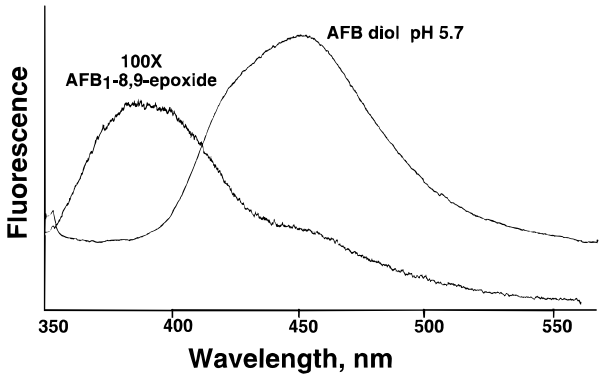

Figure 4. Fluorescence spectra of AFB *exo*-8,9-epoxide and the hydrolysis products AFB diol and AFB dialdehyde. Excitation was at 328 nm. The AFB_1 *exo*-8,9-epoxide concentration was 4.7 μM and the spectrum was recorded at 0.1X sensitivity for AFB diol (0.47 μM). The λ_{max} of the AFB 8,9-epoxide is 380 nm and the λ_{max} of the AFB diol is 452 nm.

pH Rate Profile. Hydrolysis was done in buffers of various pH and the rate of fluorescence change was determined (Figure 6). A pH-independent rate of hydrolysis of 0.59 s^{-1} was observed from pH 10.8 to about pH 5. The pseudo-first-order rate of reaction of the epoxide with H_2O is, therefore, 0.59 s^{-1} under these conditions of 7 μM AFB_1 *exo*-8,9-epoxide. At pH values <5, the log of k_{obs} is inversely related to pH with a slope of nearly −1, indicating the predominance of acid-catalyzed

(31) Larsson, P.; Pettersson, H.; Tjälve, H. *Carcinogenesis* **1989**, *10*, 1113−1118.

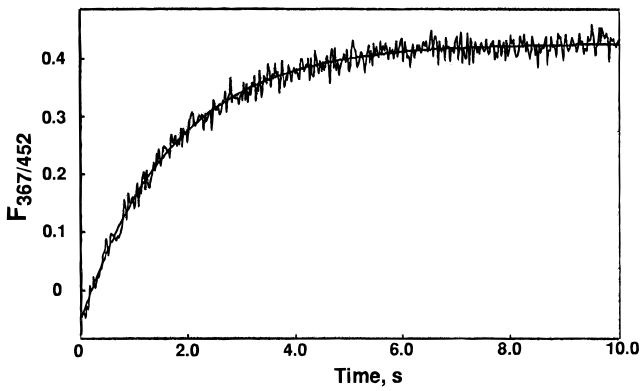

Figure 5. Time dependence of fluorescence increase ($F_{367/452}$) during AFB_1 *exo*-8,9-epoxide hydrolysis. The curve fit to the data is single exponential and the equation is $Y = A_0e^{-kt} + B$ where k is k_{obs} (0.60 ± 0.004 s^{-1}). Hydrolysis was done in buffer (pH 7.0) at 25 °C with an AFB_1 *exo*-8,9-epoxide reaction concentration of 14 μM and an $(CH_3)_2$-CO final concentration of 9% (v/v).

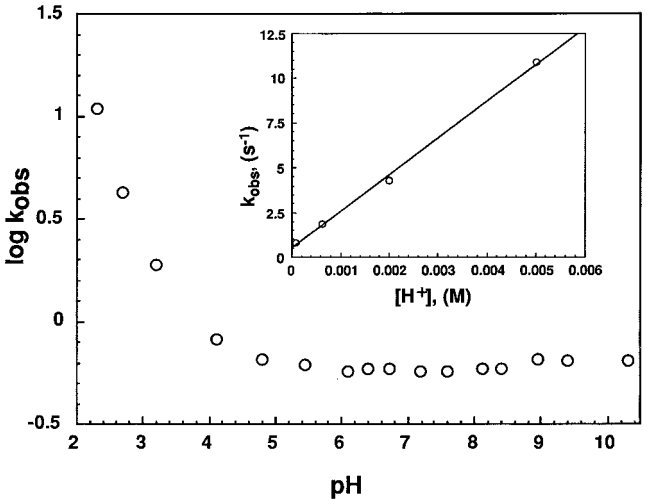

Figure 6. Logarithmic plot of AFB_1 *exo*-8,9-epoxide hydrolysis rates versus pH. Rates were determined as in Figure 5, except the final concentration of AFB_1 *exo*-8,9-epoxide was 7 μM. The inset shows the dependence of the observed rate of acid-catalyzed hydrolysis (k_{obs} on protium ion concentration (a_H+). The data are fit to the linear equation $k_{obs} = k_{H^+}a_{H^+} + k_o$ where k_{H^+} is the bimolecular acid-catalyzed rate of hydrolysis (2.1×10^3 M^{-1} s^{-1}). k_o is the spontaneous rate of hydrolysis (calculated value 0.53 s^{-1}). The spontaneous rate remains essentially constant to a pH of 10.8, the highest pH examined.

mechanisms for hydrolysis. In this range of pH the rate data for hydrolysis fit to the equation

$$k_{obs} = k_{H^+}a_{H^+} + k_o$$

where k_{H^+} and k_o are rate constants for acid-catalyzed and spontaneous reactions, respectively, and a_{H^+} is the hydrogen ion activity as measured by pH electrodes (Figure 6, inset). Hence, the bimolecular rate constant for acid-catalyzed hydrolysis is 2×10^3 M^{-1} s^{-1} and the calculated spontaneous reaction with water is 0.53 s^{-1} under these conditions. This indirectly determined spontaneous rate is within experimental error of the directly measured rate.

Base-Catalyzed AFB Dialdehyde Formation. The reversible bathochromic shift seen under basic conditions indicates that the hemiacetal AFB_{2a} ring opens at the furan rings resulting in the phenoxy anion and aldehydes.[16] AFB diol is also in equilibrium with AFB dialdehyde in mildly basic conditions. Therefore, absorbance spectra of the hydrolyzed product were determined in acidic and basic conditions: AFB diol has a λ_{max} of 365 nm and AFB dialdehyde has a greater absorbance with a λ_{max} of 395 nm, red-shifted by 30 nm (Figure 7). Since the difference in absorbance between 405 and 430 nm indicates the relative amount of dialdehyde in solution, spectra were determined in a titration through a range of pH. The difference $\Delta A_{405-430}$ was then plotted versus pH to provide a profile of the relative amount of AFB dialdehyde over the range of pH (Figure 8). A sigmoidal curve fit to these data yielded a pK_a of 8.17 ± 0.10 for the equilibrium between AFB diol and AFB dialdehyde.

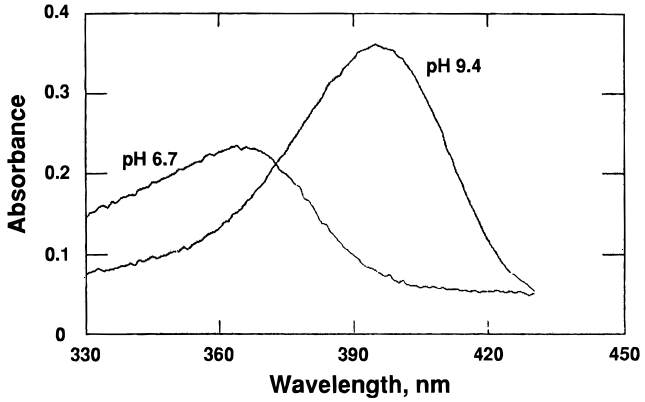

Figure 7. UV/vis spectra of AFB diol at pH 6.7 and AFB dialdehyde at pH 9.4. AFB diol exhibits a λ_{max} of 365 nm and that of AFB dialdehyde is 395 nm. Concentrations of AFB diol and AFB dialdehyde were 14 μM.

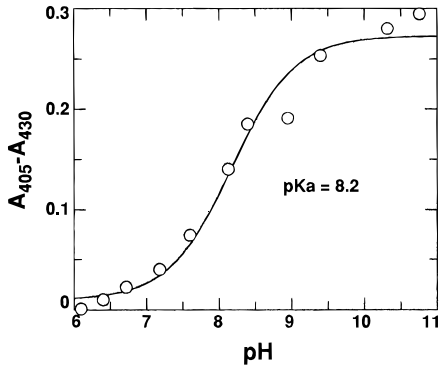

Figure 8. pH dependence of $\Delta A_{405-430}$. The difference in absorbance at 405 and 430 nm represents the relative amount of dialdehyde (Figure 7); therefore the pH dependence of this difference yields the apparent pK_a of the conversion of AFB diol to AFB dialdehyde. The data were analyzed by curve fitting to a sigmoidal function $y =$ [lim 10 exp(pH $-$ pK_a)]/[10 exp(pH $-$ pK_a) + 1], yielding a pK_a of 8.17 ± 0.10.

The increase in absorbance of AFB diol at 400 nm at more basic pH values can easily be monitored and exhibits single exponential kinetics. The relationship for a single exponential rate of decay, $[A]_t = [A]_oe^{-kt}$, converts to a linear equation, $\ln[A]_t = -kt + \ln[A]_o$, and a plot of $\ln([A]_o - [B]_t)$ versus t has a slope of $-k$, the observed rate of the reaction. This rate was dependent on pH and was determined over a pH range of 7.87−9.73. The bimolecular rate of base-catalyzed dialdehyde formation can be determined by plotting the k_{obs} versus the concentration of the hydroxide ion (Figure 9) and determining the slope of the line, yielding 2.3×10^3 M^{-1} s^{-1}. At the higher pH values a distinct second phase could be seen (e.g., in <1 min at pH 9.58), in which the absorbance continues to increase at 400 nm.

Characterization of AFB Diol and AFB Dialdehyde Structures. The assignment of the NMR spectrum of AFB diol has apparently never been reported. The spectrum was recorded in dry DMSO-d_6 (Figure 10A). The assigments (Scheme 2)

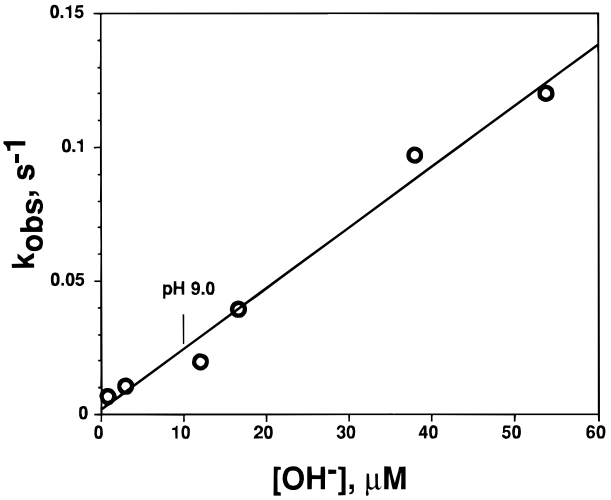

Figure 9. Dependence of the observed rate (k_{obs} of base-catalyzed conversion of AFB diol to AFB dialdehyde on [OH^-]. The data are fit to the linear equation: $k_{obs} = k_{OH^-}[OH^-]$ where k_{OH^-} is the bimolecular base-catalyzed rate of hydrolysis, 2.3×10^3 M^{-1} s^{-1}.

Scheme 2. ^{1}H NMR Assignments for AFB_1 Diol.

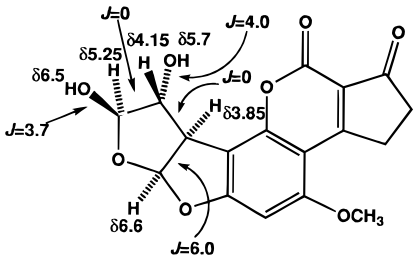

were established by decoupling experiments in which H6a, 8-OH, and 9-OH were irradiated and by deuterium exchange of the hydroxyl groups, which caused the expected simplification of signals assigned to H8 and H9. The assignments are consistent with the spectrum of the *trans* isomer 8-methoxy-9-hydroxy AFB_1 formed by uncatalyzed methanolysis of AFB epoxide reported previously.[7] In particular, the failure to observe coupling between H8 and H9 and between H9 and H9a is consistent with *trans* orientation of the protons such that in a 5-membered ring the torsional angles are near 90°.

An NMR sample of AFB diol in dry DMSO-d_6 was treated with ~1 μL of 1,8-diazabicyclo[5.4.0]undec-7-ene (DBU). The solution immediately became intensely yellow followed by a very slow darkening of the solution. The ^{1}H NMR spectrum was initially complex after addition of the DBU but showed that within 30 min the material was largely converted to two new substances having aldehyde protons near 9.5 ppm (Figure 10B).

The results are interpreted as base cleavage of the two furan rings of the AFB diol to form the dialdehyde; the resulting phenoxy anion is stabilized by delocalization into the two carbonyl groups. The DBU caused a slower loss of H_2O to give the *E* and *Z* isomers of the $\Delta^{9,9a}$ dehydration product (AFB numbering) in ~2:1 ratio. Both species have two aldehyde protons. In the major isomer, a doublet at δ 9.49 ($J = 8$ Hz), assigned to H8, is coupled to a doublet at δ 6.4, assigned to H9. The other aldehyde signal, H6a, is a sharp singlet at δ 9.52. In the minor isomer, H6a′, H8′, and H9′ appeared at δ 9.72, 9.75 (d), and 6.72 (d), respectively, with $J_{8,9} = 8$ Hz. The assigned couplings were confirmed by homonuclear decoupling.

A complication in the spectra was that some deuterium exchange of H9 occurred (due to trace contamination of the DMSO-d_6 with D_2O or direct transfer from the DMSO-d_6). This caused the doublets for H8 in the two isomers to be gradually converted to singlets. A second complication was that the sample gradually degraded, probably due to base-catalyzed air oxidation. In spite of these problems the spectra could be observed for at least 24 h. However, the instability made it impossible to obtain NOE difference spectra needed to individually assign the geometrical configurations of the two species.

Attempts to recover neutral forms of the $\Delta^{9,9a}$ species were unsuccessful. We were unable to observe discrete species after acidification. A separate experiment was carried out in which AFB diol was treated with K_2CO_3 in H_2O, lyophilized, and then taken up in DMSO-d_6; the sample failed to give a defined spectrum and it is believed that decomposition had occurred.

Recovery of AFB Diol from AFB Dialdehyde. AFB_1 epoxide was hydrolyzed at pH 7 and promptly acidified with acetic acid and injected onto an HPLC system (see Methods); >85% of the absorbance of eluted compounds was due to the AFB diol ($t_R = 7.85$ min). No detectable product with $t_R = 6.6$ min was seen. However, incubation of the epoxide for 20 min at pH 9.9 produced a product eluting at 6.6 min that constitutes about 9% of total A_{365}. Therefore, there appears to be a slow production of a slightly more hydrophilic product at comparatively high pH (9.9). The UV/vis and fluorescence

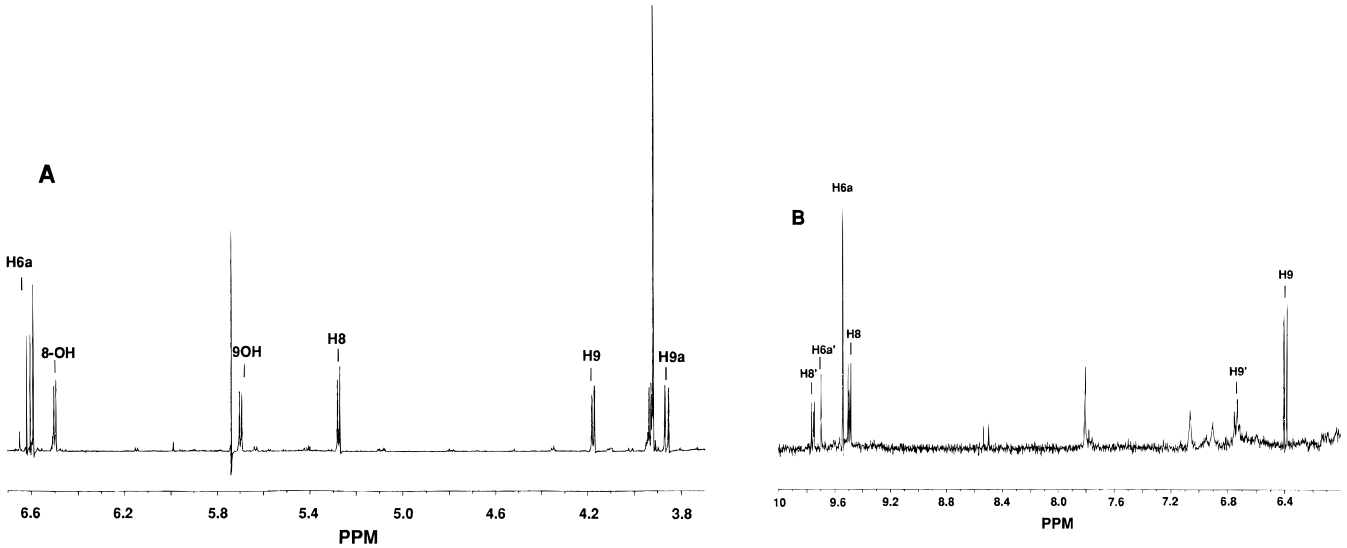

Figure 10. ^{1}H NMR spectra (400 MHz) of AFB diol in DMSO-d_6 (A) and dehydrated AFB dialdehyde in DMSO-d_6 and ~1 μL of DBU (B). The assignments (Scheme 2) were established by decoupling experiments.

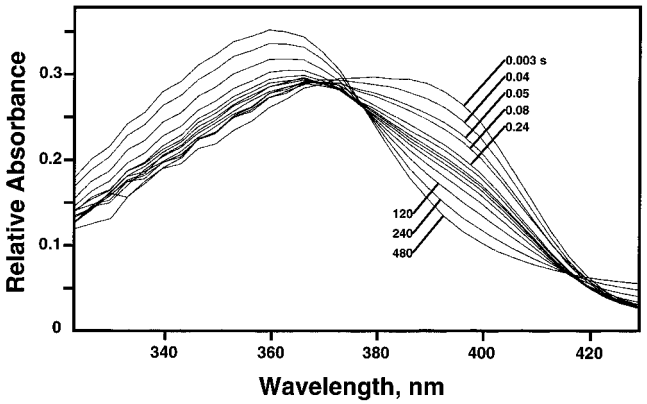

Figure 11. Multiple absorbance spectra acquired by photodiode array spectroscopy for mixing AFB dialdehyde and acidic buffer. The pH was changed by rapidly mixing a solution of 14 μM AFB diadehyde in 1.0 mM CHES solution (pH 9.6) with a 10-fold excess of 100 mM MES buffer (pH 5.7). The first spectrum was completed in 2.56 ms and the frequency of acquistion is logarithmically less frequent over the course of 500 s total time. Therefore, the first few spectra were collected more frequently than the last several, as labeled. Only selected spectra are displayed to permit distinction between them. The second isosbestic point is at 375 nm with the first one about 8 nm less. Individual slices of kinetic changes in absorbance data are shown in Figure 12.

spectra of the peak eluting at $t_R = 6.6$ min were identical to those of AFB diol.

When similar experiments were performed in an aprotic system (DMSO with DBU) there was no detectable product (A_{365}) eluted within 30 min (after a comparatively small amount of some significantly more hydrophilic products eluting at 3−4 min). This may be the result of polymerization of the aldehyde species to polymers that bind tightly to the octadecylsilane column.

Kinetics of Conversion of AFB Dialdehyde to AFB Diol. AFB dialdehyde (in 1 mM CHES buffer, pH 9.6) was added to a 10-fold volume of pH 5.7 buffer (100 mM MES). At pH 9.6 the compound is essentially in the dialdehyde form (equilibrium has a pK_a of about 8.2, *vide supra*) and the absorbance spectrum has a λ_{max} of 395 nm. The last spectrum recorded in the reaction is characteristic of AFB diol, with a λ_{max} of 360 nm, and is reached exponentially (Figure 11). The first spectrum has the λ_{max} near that of the dialdehyde, i.e. 380−390 nm, although the absorbance is much less than expected. The absorbance of the first spectrum at 390 nm is less than the maximum absorbance of the last spectrum, whereas in Figure 7 the maximum absorbance of AFB dialdehyde is about 1.5 times that of the diol spectrum.

Clearly the initial change is significantly faster and slightly different than the rest. The slow increase of A_{360} is concomitant with the decrease at 400 nm (Figure 12). The observed single exponential rate for this change is 0.01 s^{-1} (i.e., 5.8 min^{-1}). The fast phase (Figure 12, inset) is largely complete in about 0.5 s, with a rate of 12 s^{-1}. Moreover, the amplitude of the change in A_{400} is three times greater than A_{360} in the 0.5 s phase, whereas the magnitude of change at 360 nm is about 20% larger than that at 400 nm in the slow phase. The fast phase at 400 nm is at least biphasic and much of the change is occurring in the mixing time of the device (i.e., A_{400} begins < A_{360}, distinctly the reverse of the extinction coefficients of the two tautomers shown in Figure 7).

The rate limiting step of this reaction, AFB dialdehyde to AFB diol, was 0.005 s^{-1} at pH 7.2. Hence, there is a slight dependency on pH for the acid-catalyzed conversion of AFB dialdehyde to AFB diol since the rate is roughly half when the concentration of hydronium ions is reduced by 30-fold (pH 5.7 to 7.2).

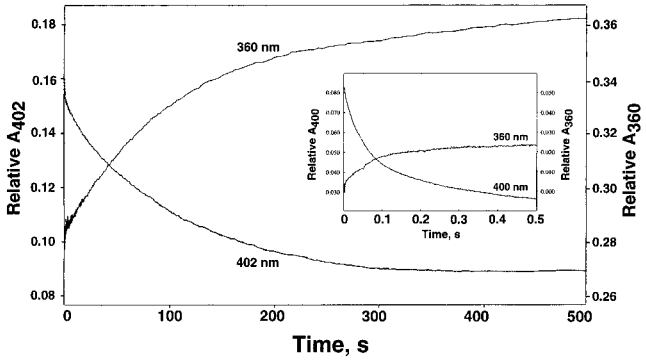

Figure 12. Time dependence of ΔA_{360} and ΔA_{402} for mixing AFB dialdehyde and acidic buffer. The absorbance of the two curves is on the same relative scale but the absolute scale is shifted and is displayed on the left and right axis for A_{402} and A_{360}, respectively, as the A_{402} begins < A_{360}. The curve fit to the data is single exponential and the equation is $Y = A_0e^{-kt} + B$ where k is k_{obs} (0.0098 ± 0.0001 s^{-1}). Although the rates at each wavelength agree, the amplitude of change at 360 nm is 20% larger than that at 402 nm. The reaction was performed as in Figure 11. The inset shows the reaction in which absorbance was monitored at these wavelengths at a 10^3-fold shorter time interval (k = 12 s^{-1}).

Scheme 3. Mechanism of Hydrolysis of AFB_1 8,9-Epoxide.

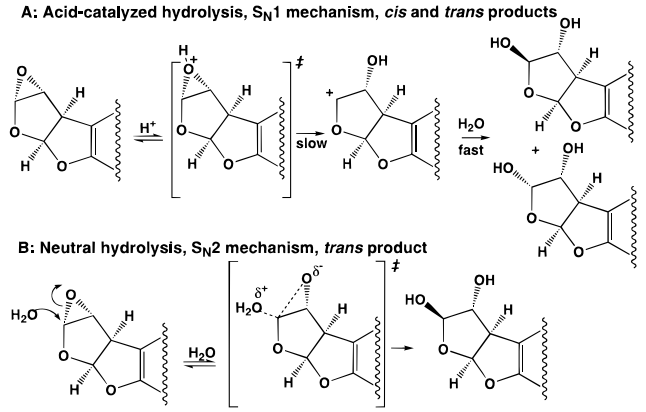

Discussion

AFB_1 *exo*-8,9-Epoxide Hydrolysis. Ever since AFB_1 epoxide was first synthesized, it has been known to be highly reactive and unstable in H_2O.[21] The $t_{1/2}$ was suggested to be ∼5−10 s.[9] We now find that the *exo* epoxide is even more reactive than suspected, with a $t_{1/2}$ of ∼1 s in 91% H_2O at 25 °C, thus making it one of the most reactive of all biologically relevant epoxides. The determination of this rate will now permit analysis of rates of conjugation with DNA and GSH and H_2O via epoxide hydrolase.

The reaction rate increases linearly with a direct dependence on proton concentration at pH <5, indicating bimolecular acid-catalyzed hydrolysis. In the pH-independent range of spontaneous hydrolysis all of the buffers gave the same k_{obs}, indicating that there is no significant effect of these nucleophiles.[32] The NMR spectrum revealed that the hydrolysis at pH 5.7 resulted in only *trans* AFB diol. This result is consistent with a concerted S_N2 mechanism shown in Scheme 3, although a mixture with some *cis* product may have converted to a

(32) Ross, A. M.; Pohl, T. M.; Piazza, K.; Thomas, M.; Fox, B.; Whalen, D. L. *J. Am. Chem. Soc.* **1982**, *104*, 1658−1665.

potentially more favorable *trans* product (*vide infra*). The H_2O oxygen is a nucleophile that attacks exclusively the more electrophilic oxirane carbon linked to the electronegative heteroatom. This leads to a transition state in which the carbon is pentacoordinate (partially cationic) and the oxirane oxygen becomes electron-rich or partially anionic. This transition state collapses to the product AFB diol.

The dependence of the rate on pH has a slope of −1 at pH <5, indicating the predominance of an acid-catalyzed mechanism for hydrolysis in this pH range. The mixture of *cis* and *trans* products from acid-catalyzed methanolysis[7] and product mixtures in many other examples[32] suggests the intermediacy of a relatively free cation, providing strong evidence for a reaction proceeding via an S_N1 mechanism in which a unimolecular step follows the bimolecular (second order) proton bonding transition state (Scheme 3A). Proton transfer to the epoxide oxygen can lead to rate-determining ring opening [or carbon−oxygen bond cleavage], thus forming the carbocation at the C8. This intermediate is comparatively short-lived but can produce both the *cis* and *trans* products. The rate constant for this reaction, 2×10^3 M^{-1} s^{-1}, is about twice that of the benzo[*a*]pyrene diol-epoxide isomer that is most reactive via acid catalysis.[33] This pathway may be relevant to reaction with DNA, since there is evidence that DNA has an acidic microenvironment[15] and catalyzes the substitution of epoxides via acid catalysis.[14]

It is interesting to note that the mutagenic relationship of the enantiomers of AFB_1 8,9-epoxide, *exo* and *endo*, is quite the opposite of at least six different multicyclic diol epoxides. In the cases of benzo[*a*]pyrene diol epoxide,[33] benzo[*c*]phenanthrene diol epoxide, chrysene diol epoxide,[34] dibenz[*a*,*j*]anthracene diol epoxide, dibenz[*c*,*h*]acridine diol epoxide,[35] and phenanthrene diol epoxide[36] the *syn* isomer is roughly an order of magnitude more reactive than the *anti* via spontaneous hydrolysis. However, the *anti* is generally more mutagenic than the *syn*,[37] which contrasts with the only mutagenic isomer of AFB_1 8,9-epoxide (*exo*) being ∼40-fold more reactive at neutral pH. The difference may be attributed to the unique and complex role that conformation contributes to benzo-ring bay-region diol epoxides reactivity[38] and the role of intercalation and orientation of AFB_1 *exo* 8,9-epoxide in DNA.[7]

Rearrangement of AFB Diol to AFB Dialdehyde. The distinct visible spectra of AFB diol and AFB dialdehyde permited the determination of kinetics for interconversion between them. The conversion to the dialdehyde is base catalyzed, with a concerted mechanism or one in which proton removal results in a short-lived intermediate (e.g., initial hemiacetal cleavage). The bimolecular rate of 2.3×10^3 M^{-1} s^{-1} results in a very slow rate of conversion, 5×10^{-4} to 1×10^{-3} s^{-1}, at physiological pH (7.5).

Although the pK_a for the interconversion of AFB diol and AFB dialdehyde had long been considered to be about 7.0−7.4,[17] we estimate this to be ∼8.2 (Figure 8), significantly higher and suggesting a minor dialdehyde population at physiological pH. The conversion of the dialdehyde back to the diol involves a rate-limiting, slightly pH-dependent step occurring at 0.01 s^{-1} (Figure 12). The reaction is clearly multiphasic with a step occurring partly in the 3 ms dead time of the stopped flow instrument. The very fast step(s) probably involves proton binding to the oxyanion (Scheme 4) but could also involve rearrangement of tautomeric structures. Proton binding to the aldehyde oxygens results in more electrophilic carbonyl carbons, hence catalyzing hemiacetal formation.

Scheme 4. Proposed Mechanism of Conversion of AFB Dialdehyde to AFB Diol.

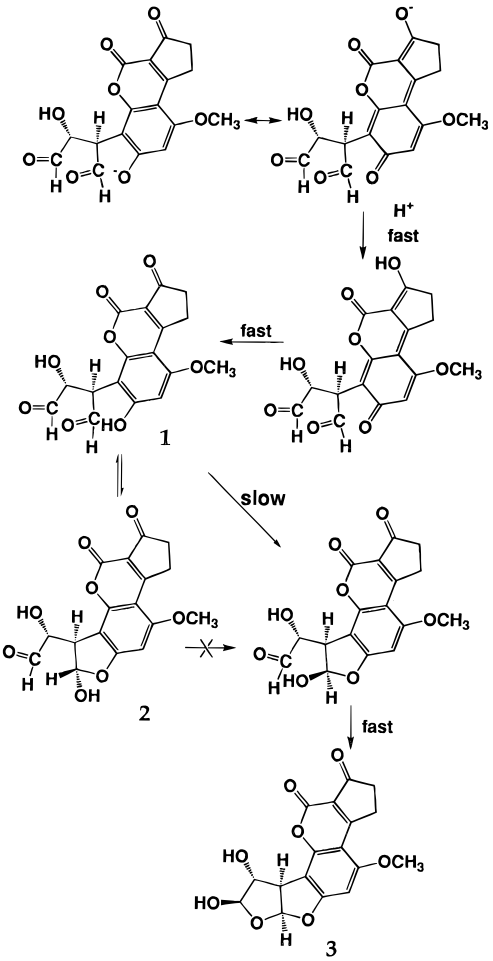

A possible mechanism of conversion of AFB dialdehyde to AFB diol is shown in Scheme 4. The first step, occurring in <3 ms, is postulated to involve rapid protonation of the phenoxy anion. Three spectrally distinct species are seen (Figure 11), and the rates for conversion can be estimated from the kinetic traces (Figure 12). The first species (**1**) is formed in <3 ms ($k > 10^3$ s^{-1}) and has a broad λ_{max} at 380 nm (protonated phenoxy compound). This changes to the second species (**2**) with λ_{max} 365 with a rate of ∼12 s^{-1} (Figure 12). The λ_{max} 365 species changes to the final product AFB diol, with a rate of 0.01 s^{-1} at pH 5.7 (Figure 12). **2** is postulated to be the thermodynamically favored *trans* ring-closed hemiacetal. This *trans* product is unable to form AFB diol because it is sterically precluded from undergoing a second cyclization and is also less likely to convert to the *cis* hemiacetal than convert to **1**. The *trans* hemiacetal (**2**) undergoes slow (rate limiting) epimerization, analogous to carbohydrate anomerization (via **1**), and the resulting *cis* hemiacetal rapidly closes to form AFB diol.

When AFB_1 *exo*-8,9-epoxide was hydrolyzed at acid pH (3.5), the ^1H NMR spectrum showed only *trans* AFB diol. This result is considered to reflect equilibration of the putative *cis* to the thermodynamically favored *trans* form (**2**, Scheme 4), with

(33) Whalen, D. L.; Montemarano, J. A.; Thakker, D. R.; Yagi, H.; Jerina, D. M. *J. Am. Chem. Soc.* **1977**, *99*, 5522−5524.
(34) Sayer, J. M.; Yagi, H.; Croisy-Delcy, M.; Jerina, D. M. *J. Am. Chem. Soc.* **1981**, *103*, 4970−4972.
(35) Sayer, J. M.; Lehr, R. E.; Kumar, S.; Yagi, H.; Yeh, H. J. C.; Holder, G. M.; Duke, C. C.; Silverton, J. V.; Gibson, C.; Jerina, D. M. *J. Am. Chem. Soc.* **1990**, *112*, 1177−1185.
(36) Whalen, D. L.; Ross, A. M.; Yagi, H.; Karle, J. M.; Jerina, D. M. *J. Am. Chem. Soc.* **1978**, *100*, 5218−5221.
(37) Wong, L.; Pack, G. R. *Int. J. Quantum Chem.* **1992**, *19*, 1−14.
(38) Sayer, J. M.; Whalen, D. L.; Friedman, S. L.; Paik, A.; Yagi, H.; Vyas, K. P.; Jerina, D. M. *J. Am. Chem. Soc.* **1984**, *106*, 226−233.

epimerization at H8 via cleavage of the hemiacetal. This epimerization was blocked in a previous experiment in which acidic methanolysis was done.[7] As a consequence of the rapid equilibration of the *cis* and *trans* forms of AFB hemiacetal, the stereochemistry of the diol cannot be used as an argument in favor of an S_N1 vs S_N2 hydrolysis mechanism. However, the formation of *trans* AFB diol at neutral pH and a mixture of *cis* and *trans* products at acid pH in the methanolysis studies[7] are viewed as evidence that neutral hydrolysis also occurs by an S_N2 mechanism to give *trans* product.

We do not know the structure of the minor product present after acidification of basic AFB dialdehyde, although it does have identical UV/vis and flurescence spectra to AFB diol. One possibility is that the compound is a stereoisomer arising from epimerization at H9a of the phenoxy species (Scheme 4), with the opposite configuration at the 6a/9a ring fusion (i.e., OH 9 is *endo* instead of the normal *exo*).

Conclusion. The AFB1 *exo*-8,9-epoxide is possibly the most reactive of the biologically-relevant epoxides known, and the spontaneous rate of hydrolysis determined here should allow the estimation of the relative roles of biologically relevant macromolecules to cancer-related pathways (i.e., reactions with DNA, glutathione transferase, and epoxide hydrolase).

Acknowledgment. This paper is dedicated to Professor Nelson J. Leonard on the occasion of his 80th birthday, in recognition of his many contributions to natural products chemistry. We thank Z. Deng and S. Kuchimanchi for preparing AFB_1 8,9-epoxide. This work was supported in part by the National Institutes of Health, U.S.P.H.S. grants R35 CA44353, R01 ES03755, and P30 ES00267. W.W.J. is supported in part by U.S.P.H.S. fellowship F32 ES05663.

JA960525K